Child's Nerv Syst (2001) 17:190–194

ORIGINAL PAPER

G.M. Bydder
M.A. Rutherford
F.M. Cowan

Diffusion-weighted imaging in neonates

Received: 9 February 2000

Presented at the Sixth Annual Congress and First Advanced Course of the European Society of Magnetic Resonance in Neuropediatrics, Marseille, 19–22 January 2000

G.M. Bydder (✉) · M.A. Rutherford
F.M. Cowan
The Robert Steiner
Magnetic Resonance Unit,
MRC Clinical Sciences Centre,
Hammersmith Hospital, Du Cane Road,
London W12 0HS, UK
Fax: +44-20-83833038

Abstract Diffusion-weighted imaging (DWI) can readily be performed in the neonate, although currently studies remain a few years behind those carried out on adults. DWI relies on the random diffusion of water molecules. As for the adult population, a pulsed gradient spin echo sequence (PGSE) with cardiac gating can be used to exploit the effect of diffusion on image contrast and to determine the apparent diffusion coefficient (D*) for tissues or fluids. Anisotropic properties caused by the restriction of the movement of water molecules may be demonstrated. In the neonatal brain restricted motion can be detected in both myelinated and unmyelinated white matter tracts. DWI has been used to study changes in global and focal ischaemic injury to the neonatal brain. A decreased D* may be documented after an ischaemic insult followed by a gradual increase. These changes are consistent with animal data but show a slower time course. Intervention following perinatal ischaemic injury must be started within hours. DWI detects early ischaemic injury and may therefore be a useful tool for identifying those infants who could benefit from intervention.

Keywords Magnetic resonance · Diffusion-weighted imaging · Neonate · Brain · Ischaemia

Introduction

Although paediatric diffusion-weighted imaging was performed soon after adult studies began [9, 10], there have been relatively few studies performed over the last decade, and only now is the subject receiving significant attention [1, 2, 3, 4, 5, 6, 7, 8].

In this paper we describe the techniques we have used in studies performed over the last 10 years. Normal features, changes seen in hypoxic-ischaemic injury and neonatal infarction are described, and other conditions are briefly mentioned.

Techniques

Two MR systems were used in these studies. One was a Picker prototype which was operated at 0.15 T. The other was a standard Picker HPQ system operating at 1.0 T. On the 0.15-T system a whole-body gradient coil set of 490 mm internal diameter was used for most studies, and provided a gradient strength of up to 16 mT/m. Quasispherical head receiver coils were used for all studies in this system, with the addition of padded foam to increase patient comfort and a plastic bag containing polystyrene beads, which was evacuated to assist with head fixation. The receiver coils were supported so that rocking motion with respiration was reduced. The same general type of fixation was used on the 1.0-T system.

Cardiac gating on alternate beats (or every fourth beat for rapid pulse rates) with a delay of 200–700 ms from the R wave was employed to time the pulse sequences into mid and late diastole. Images were of 128×256 matrix size except where specifically labelled 256×256. Two of four excitations were used in each study, with a slice thickness of 4–8 mm.

A pulsed gradient spin echo (PGSE) pulse sequence was used. TE values of 130 or 200 ms were used with the conventional whole-body gradient coils. We used b values of 550 or 600 mm^2/s (TE = 130 and 200 ms) as well as 1100 mm^2/s (TE = 200 ms) and 1510 mm^2/s (TE = 200 ms).

First-order gradient moment nulling was implemented in the *z* axis in the coronal, sagittal and transverse planes.

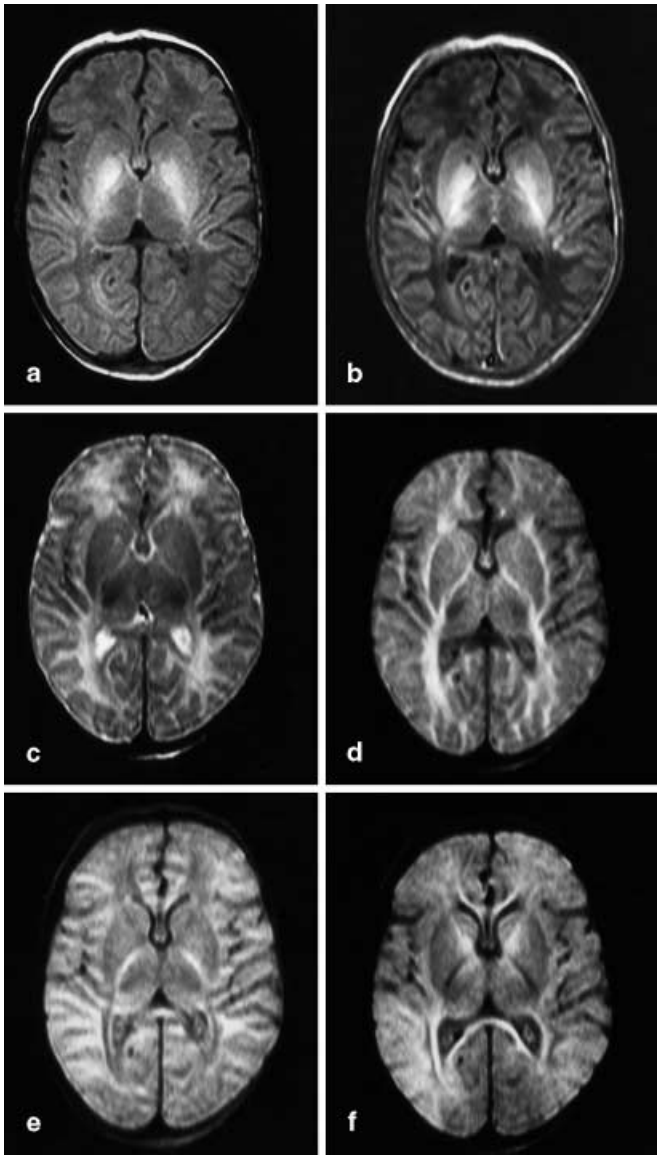

Fig. 1a–f Normal term infant. SE = 860/20 (**a**), IR = 3800/30/950 (**b**), SE = 1600/200 (**c**), SE = 1600/200/X/600 (**d**), SE = 1600/200/Y/600 (**e**) and SE = 1600/200/Z/600 (**f**) images. **a**, **b** On the T_1-weighted images, myelin is only seen in the posterior limb of the internal capsule. **d**, **e**, **f** Marked anisotropy is seen in the internal capsule. Anisotropic changes are also seen in the hemispheres, where no evidence of myelination is seen on the conventional (non-diffusion-weighted) images. This may be due to very early myelination or ordered structures in nerves

A purpose-designed small gradient coil set of 300 mm internal diameter was employed for some head studies. This set provided approximately four times the gradient strength of the standard set. With this system, it was possible to obtain b values of 550 mm^2/s with a TE of 80 ms and a diffusion time of 27 ms. The gradient set was only suitable for imaging heads and limbs in adults, although whole-body examinations of infants are possible with this system.

Unsensitised control sequences that were comparable in all respects except for the additional diffusion sensitising gradients were available to match all PGSE sequences.

Normal features

These are illustrated in Fig. 1. Anisotropic changes can be seen in the varying signal intensity in white matter. This applies both to the white matter which is myelinated and to the premyelinated areas [11].

Hypoxic-ischaemic injury

In hypoxic-ischaemic injury (HII) damage is more generalised than in focal infarction. The symptomatology of these two conditions can overlap, and both may evolve over several days, making early diagnosis and clinical grading difficult. Focal infarction generally has a good prognosis, whilst the more severe forms of HII have a very poor outcome. Cranial ultrasound and X-ray computed tomography are generally not diagnostic of either condition in the first few days of life, and conventional T1- and T2-weighted MR imaging studies have not been performed in the very early neonatal period. The need for early and accurate diagnosis in these conditions has increased, because new forms of therapy may soon be available for HII, and these are likely to require administration within 6–8 h of birth before the

Fig. 2a–r Hypoxic-ischaemic injury (HII). Examination on day 1: SE = 820/20 (**a**), IR = 3800/80/950 (**b**), SE = 1800/200 (**c**), SE = 1500/200/X/600 (**d**), SE = 1800/200/Y/600 (**e**) and SE = 1500/200/Z/600 (**f**) images. The area of abnormality is poorly demonstrated in **a**. There is evidence of more general involvement in **b** and **c**, but the changes are most obvious (high-signal areas) in the diffusion-weighted images (**d**, **e**, **f**). Examination on day 3: SE = 820/20 (**g**), IR = 3800/30/950 (**h**), SE = 1500/200 (**i**), SE = 1500/200/X/600 (**j**), SE = 1500/200/Y/600 (**k**) and SE = 1500/200/Z/600 (**l**) images. The areas of abnormality have developed a short T1 (**g**, **h**). The area of abnormality on the diffusion-weighted images **j**, **k** and **l** has decreased. Examination at 2 months: SE = 820/20 (**m**), IR = 3800/30/950 (**n**), SE = 1500/200 (**o**), SE = 1500/200/X/600 (**p**), SE = 1800/200/Y/600 (**q**) and SE = 1500/200/Z/600 (**r**) images. The brain is atrophic. The high signal areas on the diffusion-weighted images have decreased, and some anisotropic change is now apparent (**p**, **q**, **r**) ▶

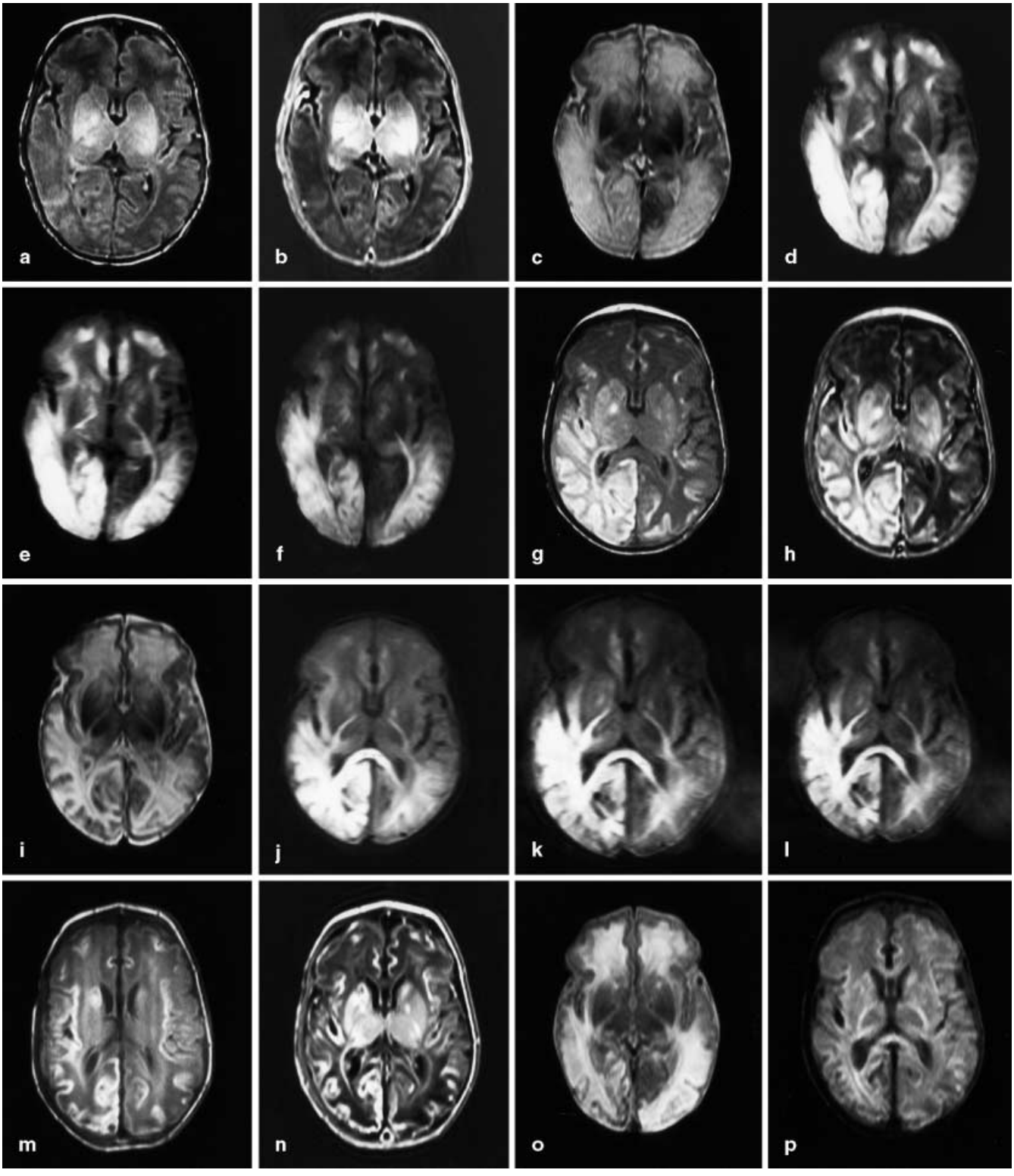

Fig. 2a–p Legend see page 191

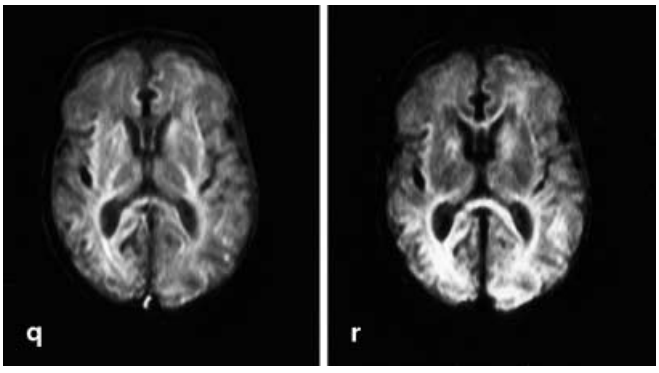

Fig. 2q, r

onset of irreversible brain damage in order to be effective.

Our findings in babies with HII (see Fig. 2) confirm an initial decrease in D* (relative signal increase) in the lesions, followed by a gradual increase in D* and changes in T1 and T2 over a period of days or weeks in

Fig. 3a–l Neonatal infarction. Initial scan on day 1: SE = 820/20 (**a**), Inversion recovery IR = 3800/30/950 (**b**), SE = 1500/200 (**c**), SE = 1500/200/X/600 (**d**), SE = 1500/200/Y/600 (**e**) and SE = 1500/200/Z/600 (**f**) images. The infarction is poorly seen in **a**, **b** and **c** but is readily seen on the diffusion-weighted images in **d**, **e** and **f**. The same patient 6 days later. SE = 820/20 (**g**), IR = 3000/30/950 (**h**), SE = 1500/200 (**i**), SE = 1500/200/X/600 (**j**), SE = 1500/200/Y/600 (**k**) and SE = 1500/200/Z/600 (**l**) images. The infarct has developed short-T1 and short-T2 components at its margins and has become more obvious on **h** and **i**. It is now much less obvious on the diffusion-weighted images (**f**, **j**, **l**)

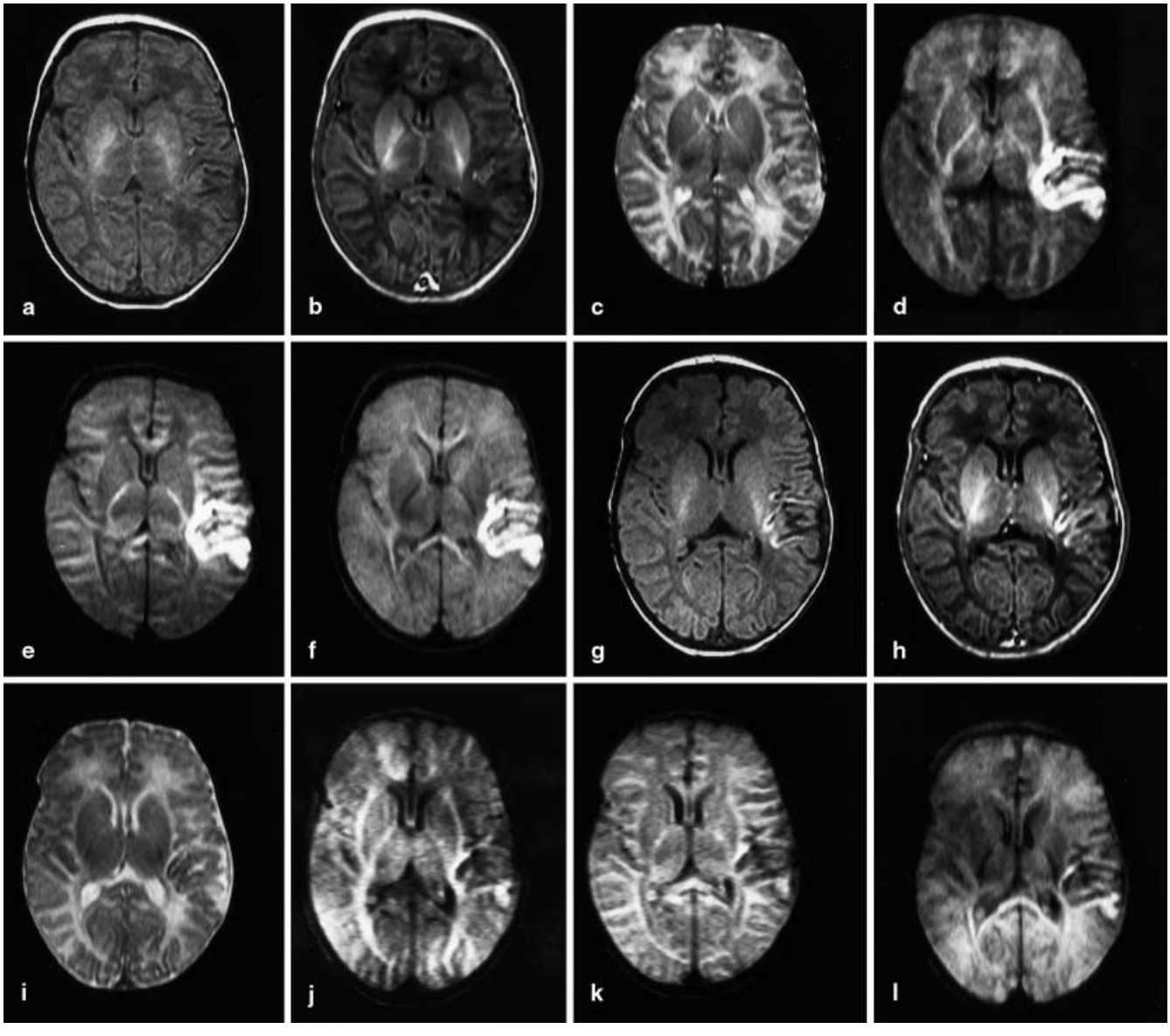

severe cases. This is consistent with animal data, though the time scale of changes is slower. We do not have a definitive explanation for this, but with animal experiments the injury is accurately timed, whereas with our infant data the injury may have occurred slowly or intermittently, and no definite timing of events is possible. This is true for both focal infarction and global injury.

Infarction

Lack of blood or oxygen to the brain may result in focal infarction with damage confined to the territory of a single artery.

Studies of stroke models of middle cerebral artery infarction in cats and of global HII in gerbils have shown that diffusion-weighted MRI can detect change within minutes of the onset of injury – which is well before conventional MRI shows changes. Areas of abnormality shown in this way subsequently become visible on conventional scans. Early changes have also been detected in acute infarction in both adults and infants (see Fig. 3). These evolve over a period of several days. Studies correlating these changes with differences in perfusion are in progress.

Animal studies have shown a reduction in the extent of the abnormality detected with diffusion-weighted imaging in stroke models following treatment with cerebroprotective agents. Diffusion-weighted MRI may be of critical importance for early diagnosis if new therapies of this type are used for treatment of HII.

Other conditions

In haemorrhage, a high signal may be seen due to restricted diffusion in the early subacute phase. In general, infections are associated with an increase in D*. Metabolic disease may produce a variable pattern, generally with an increase in D*.

Conclusion

Diffusion-weighted imaging provides a fascinating conjunction between the microscopic motion of water, the properties of myelinated nerve fibres, gross anatomy of the brain, and changes in water diffusion in disease.

More detailed study of anatomic structures will be of considerable interest, and the development of characteristic imaging planes and direction sensitisation will help in consistently obtaining images of particular tracts.

The technique is likely to be of considerable importance in detecting HII and monitoring the effects of treatment.

References

1. Barkovich AJ, Ferriero DM (1999) Line-scan diffusion imaging of term neonates with perinatal brain ischaemia. AJNR Am J Neuroradiol 20:1577–1579
2. Cowan FM, Pennock JM, Hanrahan JD, Manji KP, Edwards AD (1994) Early detection of cerebral infarction and hypoxic encephalopathy in neonates using diffusion-weighted magnetic resonance imaging. Neuropediatrics 25:172–175
3. Huppi PS, Barnes PD (1997) Magnetic resonance techniques in the evaluation of the new born brain. Clin Perinatol 24:693–723
4. Huppi PS, Maier SE, Peled S, et al (1998) Microstructural development of human newborn cerebral white matter assessed in vivo by diffusion tensor magnetic resonance imaging. Pediatr Res 44:584–590
5. Inder T, Huppi PS, Zeintara GP, et al (1999) Early detection of periventricular leukomalacia by diffusion-weighted magnetic resonance imaging techniques. J Pediatr 134:631–641
6. Neil JJ, Shiran SI, McKinstry RC, et al (1998) Normal brain in human newborns: apparent diffusion coefficient and diffusion anisotropy measured by using diffusion tensor MR imaging. Radiology 209:57–66
7. Phillips MD, Zimmerman RA (1999) Diffusion imaging in pediatric hypoxic ischaemia injury. Neuroimaging Clin N Am 9:41–52
8. Robertson RL, Ben-Sera L, Barnes PD (1999) MR line-scan diffusion-weighted imaging of term neonates with perinatal brain ischaemia. AJRN Am J Neuroradiol 20:1658–1670
9. Rutherford MA, Cowan FM, Manzur AY, et al (1991) MR imaging of anisotropically restricted diffusion in the brain of neonates and infants. J Comput Assist Tomogr 15:188–198
10. Sakuma H, Nomura Y, Takeda K, et al (1991) Adult and neonatal human brain: diffusional anisotropy and myelination with diffusion-weighted MR imaging. Radiology 180:229–233
11. Wimberger DM, Roberts TP, Barkovich AJ, et al (1995) Identification of 'premyelination' by diffusion-weighted MRI. J Comput Assist Tomogr 19:28–33